hsa_circ_0007766 regulates tumorigenesis and metastasis of breast cancer via miR-1301-3p/DNMT3B feedback loop

HUA YANG[1,2], YUAN LI[3], YUXIANG LU[4], TAO YANG[3] and YUANKUI CHU[3]

[1]School of Medical Technology, North Minzu University, Yinchuan, Ningxia Hui Autonomous Region 750021, P.R. China; [2]Ningxia Key Laboratory of Bioimaging and Intelligent Diagnostics, North Minzu University, Yinchuan, Ningxia Hui Autonomous Region 750021, P.R. China; [3]School of Medical Laboratory, Ningxia Medical University, Yinchuan, Ningxia Hui Autonomous Region 750004, P.R. China; [4]Department of Laboratory Medicine, Xi'an Third Hospital, Xi'an, Shaanxi 710016, P.R. China

Received July 14, 2026; Accepted October 2, 2026

DOI: 10.3892/mmr.2026.14078

Abstract. The development and progression of breast cancer (BC) are intricately linked to the dysregulation of non-coding RNA expression and aberrant methylation patterns. In the present study, the functional mechanism of hsa-circ-0007766 was uncovered, identifying it as an oncogenic circular RNA (circRNA) in BC. Reverse transcription-quantitative polymerase chain reaction was employed to assess the expression levels of hsa-circ-0007766, miR-1301-3p and DNA methyltransferase (DNMT) 3B in BC cell lines. Additionally, MTT, wound healing and Transwell assays were utilized to explore the roles of hsa-circ-0007766 and miR-1301-3p in cellular proliferation, migration and invasion. Protein expression was quantified using western blot analysis, while dual-luciferase reporter assays were conducted to confirm the interaction between hsa-circ-0007766 and miR-1301-3p or DNMT3B. The present findings revealed that hsa-circ-0007766 and DNMT3B are upregulated, while miR-1301-3p is downregulated in BC cell lines. Functionally, the knockdown of hsa-circ-0007766 significantly inhibited cell proliferation, migration and invasion. hsa-circ-0007766 was identified as a sponge of miR-1301-3p, and the inhibition of miR-1301-3p reversed the suppressive effects of hsa-circ-0007766 knockdown on BC progression. Moreover, DNMT3B, which is upregulated in BC, was found to be a downstream target gene of miR-1301-3p, regulating cell proliferation, migration and invasion. Notably, a positive feedback loop between miR-1301-3p and DNMT3B was observed. In conclusion, the present study demonstrated that hsa-circ-0007766 regulates cell proliferation, migration and invasion in BC cells through a miR-1301-3p/DNMT3B feedback loop. These findings offer novel insights into the molecular mechanisms underlying BC and may pave the way for the development of new diagnostic and therapeutic strategies.

Correspondence to: Professor Yuankui Chu, School of Medical Laboratory, Ningxia Medical University, 692 Shengli Street, Xingqing, Yinchuan, Ningxia Hui Autonomous Region 750004, P.R. China
E-mail: chuyuankui@163.com

Key words: breast cancer, hsa-circ-0007766, microRNA-1301-3p, DNA methyltransferase 3B, feedback loop

Introduction

Breast cancer (BC) stands as the most prevalent malignant tumor globally and accounts for a significant number of cancer-related deaths among women worldwide (1,2). The etiology and progression of BC are highly complex, with numerous studies implicating non-coding RNAs (ncRNAs), including circular RNA (circRNA), microRNA (miRNA or miR), and the epithelial-mesenchymal transition, in its development (3-5). CircRNA, characterized by their covalently closed loop structure, are known to contribute to cancer progression through various mechanisms, such as sponging miRNA, RNA-binding proteins and protein translators (6-8). An increasing number of circRNAs have been investigated to further explore the mechanism underlying the biological processes of BC (3,9,10).

In the present study, focus was addressed on the circRNA hsa_circ_0007766, found through GEO datasets as a product of exon cyclization from the gene erb-b2 receptor tyrosine kinase 2 (ERBB2, chr17:37864573-37866734). The present investigation builds upon previous research highlighting hsa_circ_0007766's role in various cancers, where it has been shown to modulate the key cell cycle proteins such as Cyclin D1, Cyclin E1 and CDK4, thereby promoting the malignant proliferation of lung adenocarcinoma (11). Hsa_circ_0007766 could regulate gastric cancer progression through the miR-1233-3p/GDF15 axis (12). Li *et al* (13) further explored the coding potential of circ-HER2 (hsa_circ_0007766), revealing that the peptide HER2-103, encoded by Circ-HER2, is expressed in some triple-negative BC cases and can enhance cell proliferation, invasion and tumorigenicity *in vitro* and *in vivo*.

The circRNA/miRNA/mRNA axis may be a molecular marker for the early diagnosis and prognosis of BC (14). The current research suggests that hsa_circ_0007766 may also function as a miRNA sponge, facilitating tumorigenesis.

Upregulation of hsa_circ_0007766 was observed in BC cells and bioinformatics was utilized to predict its target miRNAs and the subsequent target mRNAs of the miRNAs. The present findings confirm that hsa_circ_0007766 modulates DNA methyltransferase (DNMT) 3B through miR-1301-3p sponges, thereby promoting BC cell proliferation, migration and invasion. Collectively, the present study not only sheds new light on the pathogenesis of BC but also expands our comprehension of hsa_circ_0007766's mechanisms, positioning it as a potential diagnostic biomarker and therapeutic target for BC.

Materials and methods

Cell culture. Human BC cell lines MCF-7 was procured from the American Type Culture Collection, while MCF-10A (cat. no. 1101HUM-PUMC000406), MDA-MB-231 (cat. no. 1101HUM-PUMC000014), MDA-MB-453 (cat. no. 3101HUMSCSP5044), HCC38 (cat. no. 1101HUM-PUMC000220) and BT-549 (cat. no. 3101HUMSCSP5397) were sourced from the National Experimental Cell Resource Sharing Platform. MCF10A was cultured using the MEGM Bullet Kit (cat. no.CC-3150; Lonza Group, Ltd.) supplemented with 10% fetal bovine serum (FBS) (cat. no. ST30-3302P; PAN-Biotech GmbH) and 100 ng/ml cholera toxin (cat. no. C8052; MilliporeSigma). MCF-7, MDA-MB-231 and MDA-MB-453 were maintained in DMEM medium (cat. no. SH30243.01B; Hyclone; Cytiva) with 10% FBS and 1% penicillin/streptomycin (cat. no. SV30010; Hyclone; Cytiva). HCC38 and BT-549 were cultured in RPMI-1640 medium (cat. no. SH30809.01B; Hyclone; Cytiva) containing 10% FBS and 1% penicillin/streptomycin. All cultures were incubated at 37˚C with 5% CO_2.

Bioinformatics analysis. The Gene Expression Omnibus (GEO) database was utilized to analyze the expression profiles of 21 BC-related circRNAs (GSE101123). Differential gene expression heat maps were constructed using the pheatmap software package (http://www.heatmapper.ca/expression/), with a significance threshold of $P<0.05$ and $|\log2 (\text{fold change})|>1$ for differentially expressed circRNAs. CircBase software was employed to retrieve the linear encoding genes corresponding to circRNAs. The volcano plot of differentially expressed genes was generated using tools from the Sanger box. Target miRNAs with binding sites to circRNA were analyzed and predicted using starBase (http://starbase.sysu.edu.cn/), miRanda database (http://www.microrna.org/microrna/home.do), and RNAhybrid (http://bibiserv.techfak.uni-bielefeld.de/rnahybrid/). The Bioinformatics & Evolutionary Genomics software (http://bioinformatics.psb.ugent.be/webtools/Venn/) was used to create Venn diagrams. Target genes of miR-1301-3p were predicted by Starbase, PITA (http://genie.weizmann.ac.il/pubs/mir07/mir07_data.html), miRTarBase (http://mirtarbase.mbc.nctu.edu.tw/index.html), PicTar (http://www.pictar.org/), TargetScan (http://www.targetscan.org/).

Semiquantitative reverse transcriptase PCR (RT-PCR) and reverse transcription-quantitative polymerase chain reaction (RT-qPCR). Total RNA was isolated using TRNzol reagent [cat. no. DP424; Tiangen Biotech (Beijing) Co., Ltd.], and cDNA was synthesized with the HiScript® Q RT SuperMix for qPCR (+gDNA wiper) Kit (cat. no. R223-01; Vazyme Biotech Co., Ltd.) following the manufacturer's protocol. RT-PCR was conducted using the Golden Easy PCR System (cat. no. KT221; Tiangen Biotech Co., Ltd.) in a 20-μl reaction system, under the following reaction conditions: 94˚C for 5 min; followed by 35 cycles at 94˚C for 15 sec, 58˚C for 15 sec, 72˚C for 15 sec and then 72˚C for 15 min. The PCR products were visualized by 2% agarose gel electrophoresis (AGE). RT-qPCR was performed with ChamQ SYBR qPCR Master Mix Kit (cat. no. Q311; Vazyme Biotech Co., Ltd.), and relative expression levels were calculated using the $2^{-\Delta\Delta Cq}$ method (15). GAPDH served as an internal control for hsa-circ-0007766 and mRNAs, while U6 was used for miR-1301-3p. qPCR was performed in a 20-μl reaction system with the following thermal profile: Holding stage at 50˚C for 2 min, 95˚C for 5 min, followed by 40 cycles in the cycle stage (95˚C for 15 sec, 59˚C for 15 sec and 70˚C for 15 sec) and melt curve analysis at 95˚C for 15 sec and 59˚C for 1 min, followed by a gradual increase to 95˚C for 15 sec. Primer sequences are listed in Table SI.

Transfection. Hsa_circ_0007766 small interfering RNA (siRNA), miR-1301-3p mimic/inhibitor and DNMT3B siRNA, along with their corresponding negative controls (NC), were designed and synthesized by Guangzhou RiboBio Co., Ltd. Transfections with the target gene-specific mimics/inhibitors and siRNAs (50 nM) were carried out using Lipofectamine® 2000 (cat. no. 11668019; Invitrogen; Thermo Fisher Scientific, Inc.) according to the manufacturer's instructions. Cells were incubated with the transfection complexes at 37˚C in a humidified incubator containing 5% CO_2. After 6 h, the medium was replaced with fresh medium to continue the culture, and the culture time was determined according to the specific experiment. The sequences of the designed siRNAs targeting hsa_circ_0007766 were as follows (sense): si-hsa_circ_0007766_001, sense 5'-CTGTCCCTGATATCCAGGA-3', antisense 5'-TCCTGGATATCAGGGACAG-3'; si-hsa_circ_0007766_002, sense 5'-TGCCTGTCCCTGATATCCA-3', antisense 5'-TGGATATCAGGGACAGGCA-3'; siRNA-NC, sense 5'-UUCUCCGAACGUGUCACGUTT-3', antisense 5'-AACUCCGAACGUGUCACGUTT-3'. The sequences of the miR-1301-3p mimics and inhibitor were as follows: miR-1301-3p mimic, sense 5'-UUGCAGCUGCCUGGGAGUGACUUC-3', antisense 5'-GAAGUCACUCCCAGGCAGCUGCAA-3', miR-NC mimic, sense 5'-UUCUCCGAACGUGUCACGU-3', antisense: 5'-ACGUGACACGUUCGGAGAA-3'; miR-1301-3p inhibitor 5'-GAAGUCACUCCCAGGCAGCUGCAA-3' and miR-NC inhibitor 5'-CAGUACUUUUGUGUAGUACAA-3'. The DNMT3B siRNA sequences were: siRNA-DNMT3B-01, sense 5'-GGACTACTTTGCATGTGAA-3', antisense 5'-TTCACATGCAAAGTAGTCC-3'; siRNA-DNMT3B-02, sense 5'-GCAACGATCTCTCAAATGT-3', antisense 5'-ACATTTGAGAGATCGTTGC-3'; siRNA-DNMT3B-03, sense 5'-CCAAGCGCCTCAAGACAAA-3', antisense 5'-TTTGTCTTGAGGCGCTTGG-3' and siRNA-NC, sense 5'-GACTTCATAAGGCGCATGC-3', antisense 5'-GCATGCGCCTTATGAAGTC-3'.

MTT assay. Cells were transfected for 6 h with siRNAs, miR-1301-3p mimic or miR-1301-3p inhibitor, and the corresponding controls. After transfection for 6 h, the cells were seeded in 96-well plates. The cells were cultured for 12 h after which MTT (20 μl) was added at 0, 24, 48, 72 and 96 h, and the cells were incubated for 4 h at 37˚C. Subsequently, the medium was replaced with DMSO to dissolve the formazan and absorbance at 492 nm was measured using a microplate reader (Thermo Fisher Scientific, Inc.).

Colony formation assay. After transfection for 6 h, cells were seeded in 12-well plates. Cultures were maintained for 2 to 3 weeks, and cell colonies were fixed with 4% paraformaldehyde for 30 min and stained with 0.1% crystal violet for 15-30 min at room temperature. An optical microscope was used to count colonies (>50 cells/colony).

Wound healing assay. After transfection for 6 h, cells were seeded in 6-well plates and cultured for 12 h. A scratch was made across the cells with a plastic pipette tip. Cells were cultured in DMEM medium containing 3% FBS and images were captured at the same scratch site at 0 and 24 h. The cell migration rate (%) was calculated as (0 h scratch width-24 h scratch width)/0 h scratch width x100.

Invasion assays. 24-well Transwell chambers (cat. no. 3421; Corning, Inc.) were used to assess cell invasion. The upper chambers were precoated with Matrigel matrix for 2 h at 37˚C. Cells were incubated with the transfection complexes for 6 h, after which the medium was replaced with fresh complete medium. Invasion assays were performed 48 h after transfection. Transfected cells ($1x10^5$ cells/well) were suspended in serum-free medium and added to the upper chamber, while medium containing 10% FBS was added to the lower chamber. After 48 h of incubation at 37˚C, cells on the upper surface of the Transwell membrane were removed with cotton swabs. Invasive cells on the lower side were fixed with methanol for 30 min at room temperature and stained with 0.1% crystal violet for 15 min at room temperature. Images of invasive cells were captured at x100 magnification, and absorbance was measured at 590 nm with a plate reader after eluting bound crystal violet with 3% acetic acid.

Dual-luciferase reporter assay. pmiR-RB-Report™-hsa_circ_0007766-WT, pmiR-RB-Report-hsa_circ_0007766-Mut, pmiR-RB-Report-DNMT3B-WT, pmiR-RB-Report-DNMT3B-Mut were constructed and synthesized by Guangzhou RiboBio co. ltd. MCF-7 cells were cultured in 96-well plates and co-transfected with wild-type or mutant-type hsa_circ_0007766 or DNMT3B and miR-1301-3p mimics or NC using Lipofectamine 2000. Cells were harvested after 48 h, and the Dual Luciferase Reporter Assay System (cat. no. E1910; Promega Corporation) was used to measure luciferase activity according to the manufacturer's instructions. Firefly luciferase activity was normalized to *Renilla* luciferase activity (firefly/*Renilla* ratio) for each well. The average relative luciferase activity of the control group was normalized to 1 and the luciferase activity of the experimental group was shown as relative fold change.

Western blot analysis. Western blot analysis was performed 48 h after transfection. Cells were lysed using RIPA lysis buffer (cat. no. P0013C; Beyotime Institute of Biotechnology), and protein concentrations were determined with the BCA Protein Assay Kit (cat. no. P0010; Beyotime Institute of Biotechnology). Total protein (40 μg) was separated by SDS-PAGE on a 10% gel and transferred to PVDF membranes, which were blocked with 5% skimmed milk powder solution for 3 h at room temperature. The membranes were then incubated with anti-DNMT3B (cat. no. 26971-1-AP; 1:1,000; Proteintech Group, Inc.) and anti-GAPDH (cat. no. 10494-1-AP; 1:1,000; Proteintech Group, Inc.) overnight at 4˚C, followed by incubation with HRP-conjugated secondary antibody (cat. no. S0001; 1:2,000; Affinity Biosciences) at room temperature for 1 h. After the ECL chemiluminescence reagent (cat. no. KGP1127; Jiangsu KeyGen Biotech Co., Ltd.) was developed, it images were captured with a gel electrophoresis imager (Beijing Sage Creation Science Co., Ltd). The gray value of protein bands was analyzed using ImageJ 1.48 (National Institutes of Health).

Statistical analysis. Statistical analyses were conducted using GraphPad Prism 8.0 software (Dotmatics). Each experiment was performed in triplicate. Data are presented as the mean ± standard deviation (SD). Differences between two groups were assessed using unpaired Student's t-test, whereas multiple groups were compared using one-way ANOVA followed by Tukey's post hoc test for pairwise comparisons. $P<0.05$ was considered to indicate a statistically significant difference.

Results

Identification and characterization of hsa_circ_0007766 in BC. The GEO database (dataset GSE101123) was leveraged to locate 21 differentially expressed circRNAs, identifying 11 that were downregulated and 10 that were upregulated, as depicted in the heatmaps (Fig. 1A). Among these, hsa_circ_0007766, which was upregulated in BC, was selected for further investigation due to its linear coding gene ERBB2 (HER2), a key factor in the onset and progression of BC. Additionally, the present analysis of differentially expressed circRNAs between BC and adjacent normal tissues using Sanger box confirmed the upregulation of hsa_circ_0007766 in BC (Fig. 1B). According to circBase, hsa_circ_0007766 is located on human chromosome 17 and is formed from exons 7-11 of ERBB2 through back-splicing, totaling 676 bp. Sanger sequencing verified the back-splicing junction (Fig. 1C). To confirm the circular structure of hsa_circ_0007766, convergent and divergent primers were employed to amplify circRNA and linear RNA from BC cell lines by RT-PCR (Fig. 1C). Gel electrophoresis results revealed that cDNA of hsa_circ_0007766 was detectable only by divergent primers, while gDNA of linear RNA was not amplified by these primers (Fig. 1D).

Hsa-circ-0007766 is high-expressed in BC cell lines and downregulated hsa-circ-0007766 inhibits the progression of BC cell lines in vitro. RT-qPCR confirmed the elevated expression of hsa_circ_0007766 in BC cells (MDA-MB-231, BT-549, MDA-MB-453 and MCF-7) compared with normal breast epithelial cells MCF-10A (Fig. 2A). To explore the biological

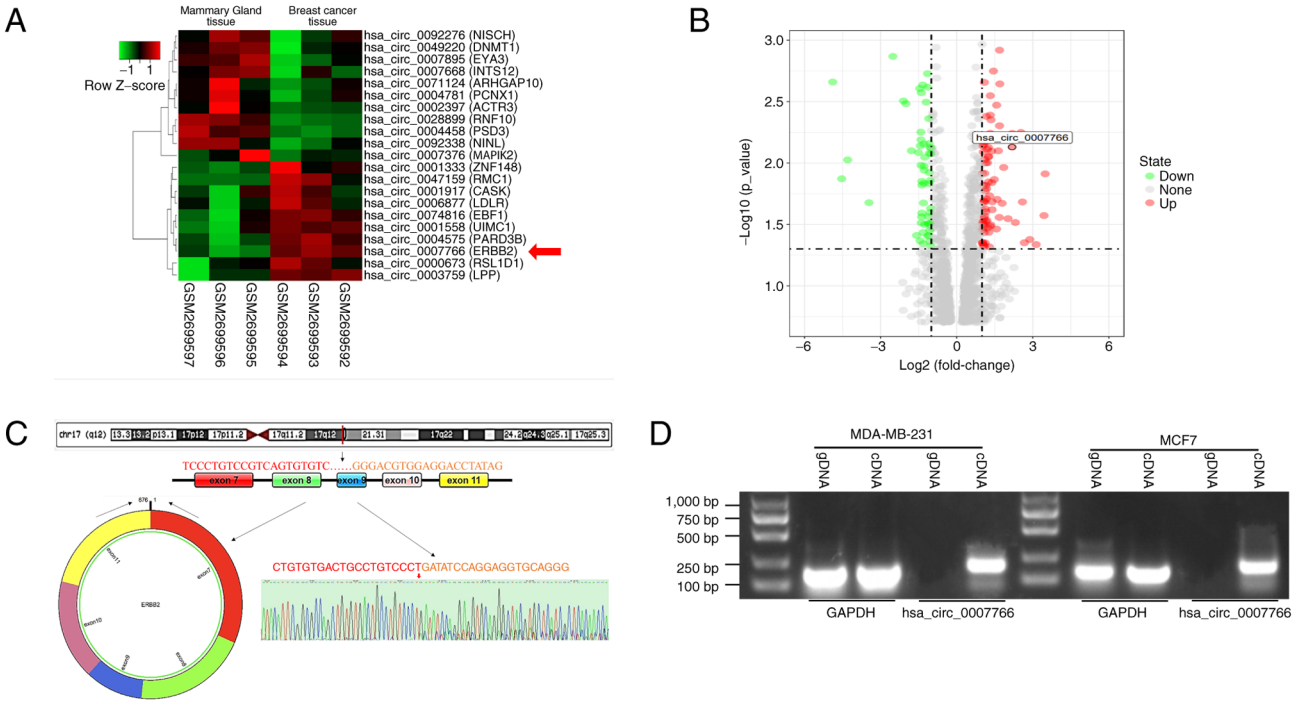


Figure 1. hsa_circ_0007766 is verified and characterized in BC cells. (A) Heatmap showed 21 representatives differentially expressed circRNAs in BC tissues (GSM2699594, GSM2699593, GSM2699592) compared with tumor adjacent normal tissues (GSM2699597, GSM2699596, GSM2699595). Red and green colors indicate upregulated and downregulated circRNAs, respectively. (B) The volcano plot illustrates the differential expression of circRNAs between BC tissues and tumor-adjacent normal tissues. The x-axis represents the log2 fold change, while the y-axis represents the-log10 P-value. (C) A schematic illustration of hsa-circ-0007766 formation through 'head-to-tail' splicing from exons 7-11 was provided. The back-splicing junction sequences were verified by Sanger sequencing, with the red arrow indicating the back-splicing junction of hsa_circ_0007766. (D) RT-PCR analysis using divergent and convergent primers confirms the presence of hsa_circ_0007766 in BC cell lines. Hsa_circ_0007766 was detectable by divergent primers from cDNA but not from gDNA. GAPDH served as a negative control. BC, breast cancer; circRNA, circular RNA.

function of hsa_circ_0007766 in BC cells, siRNAs targeting hsa_circ_0007766 were designed. RT-qPCR was used to detect the relative expression of hsa_circ_0007766 after transfection of the corresponding vectors or NC for 48 h in BC cell lines. The results showed a significant downregulation of hsa_circ_0007766 compared with the NC group (Fig. 2B). Subsequently, MTT assays, colony formation assays, wound healing assays and Transwell invasion assays were employed to assess the impact of hsa_circ_0007766 on the progression of BC cells. The results demonstrated that downregulation of hsa_circ_0007766 significantly inhibited the proliferation, migration and invasion of MCF-7 and MDA-MB-231 cell lines compared with the NC group (Fig. 2C-F). Collectively, these results elucidated a promoting role for hsa_circ_0007766 in the occurrence and development of BC.

miR-1301-3p is downregulated in BC tissues and cells and hsa-circ-0007766 acts as a miRNA sponge for miR-1301-3p. To explore the downstream miRNAs that bind to hsa_circ_0007766, 17 potential target miRNAs were predicted using starBase, miRanda database and RNAhybrid (Fig. 3A; Table SII). miR-1301-3p was selected as a candidate miRNA for subsequent experiments based on its binding site with hsa_circ_0007766. Volcano plot analysis using the GEO database revealed that miR-1301-3p was downregulated in BC tissue ($P<0.05$ and fold change >1; Fig. 3B). The expression of miR-1301-3p was also found to be downregulated in BC cell lines by RT-qPCR (Fig. 3C). The expression correlation between hsa_circ_0007766 and miR-1301-3p was then examined by RT-qPCR and it was found that the expression of miR-1301-3p was significantly upregulated after downregulation of hsa_circ_0007766 (Fig. 3D). To further verify the sponge of hsa_circ_0007766 on miR-1301-3p, the hsa_circ_0007766 luciferase reporter vector (wild-type and mutant type) for the binding site with miR-1301-3p was synthesized and constructed by Guangzhou RiboBio Co., Ltd (Fig. 3E). The dual-luciferase reporter assay results indicated that miR-1301-3p decreased the relative luciferase activity of the wild-type luciferase reporter but not the mutant one (Fig. 3F). This suggests that hsa_circ_0007766 interacts with miR-1301-3p and may act as a competing endogenous RNA (ceRNA) by targeting miR-1301-3p.

Overexpression of miR-1301-3p inhibits the progression of BC cells in vitro. To evaluate the biological function of miR-1301-3p in BC cells, miRNA mimics and inhibitors or corresponding NC constructs were designed. RT-qPCR results showed that the expression of miR-1301-3p was significantly upregulated or downregulated upon transfection with miRNA mimics or inhibitors compared with the corresponding NC group (Fig. 4A). Meanwhile, cell proliferation, colony formation, migration and invasion abilities were significantly suppressed or promoted in BC cells transfected with miR-1301-3p mimics or inhibitor compared with the corresponding NC group (Fig. 4B-E). Collectively, overexpression of miR-1301-3p was validated to suppress cell EMT,

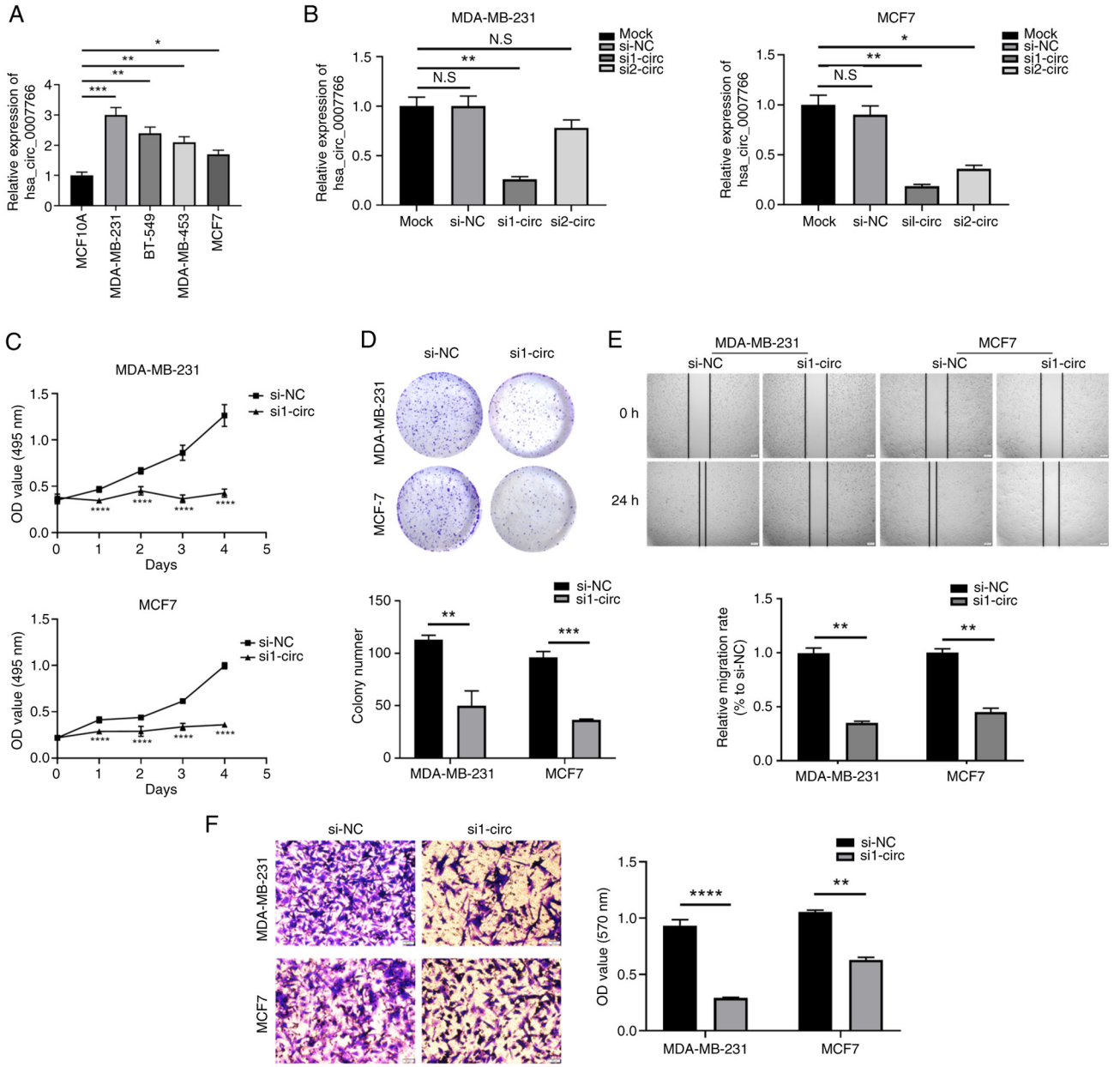


Figure 2. Hsa-circ-0007766 is high-expressed in BC cell lines and its downregulation inhibits the progression of BC cells *in vitro*. (A) The expression levels of hsa-circ-0007766 was detected in several BC cell lines and MCF10A cell lines using RT-qPCR. (B) The effective downregulation of hsa-circ-0007766 were verified in BC cells after transfection with si-hsa-circ-0007766 by RT-qPCR. (C and D) MTT assays and colony formation assays were used to detect the cell viability and colony forming ability in BC cells transfected with NC and siRNA. (E and F) Wound healing assays and Transwell Invasion assays were performed to evaluate cell migration and invasion in BC cells transfected with NC and siRNA. GAPDH served as the normalizing gene. Compared with the si-NC group, *P<0.05, **P<0.01, ***P<0.001 and ****P<0.0001. Magnification, x100. Scale bar, 100 μm. BC, breast cancer; RT-qPCR, reverse transcription-quantitative PCR; siRNA, small interfering RNA; NC, negative control; N.S., no significance.

migration and invasion, suggesting an inhibitory role for miR-1301-3p in BC.

DNMT3B is a downstream target of miR-1301-3p and reverse-regulates miR-1301-3p. To explore the downstream target genes of miR-1301-3p in BC cells, potential target genes were predicted using Starbase, PITA, miRTarBase, PicTar and TargetScan. Five candidate target genes of miR-1301-3p, including TGFBR2, smad4, DNMT3B, ARHGAP32 and Snail2, were identified by RT-qPCR. The results showed that the expression of DNMT3B was inhibited or upregulated after transfection of miR-1301-3p mimics or inhibitor in MCF7 and MDA-MB-231 cells, while the effects on other genes were not significant (Fig. 5A). Furthermore, it was observed that the methylation level of the miR-1301-3p promoter region in MDA-MB-231 and MCF7 cells was markedly higher compared with normal breast epithelial cells MCF10A, while the non-methylation level was correspondingly lower (Fig. S1). This suggests that the low expression of miR-1301-3p in BC cells is associated with methylation regulation. Therefore, DNMT3B may act as a potential downstream target gene of miR-1301-3p. RT-qPCR was used to clarify the expression of DNMT3B in BC cells, indicating that DNMT3B was upregulated in BC cell lines (Fig. 5B). Dual luciferase reporter

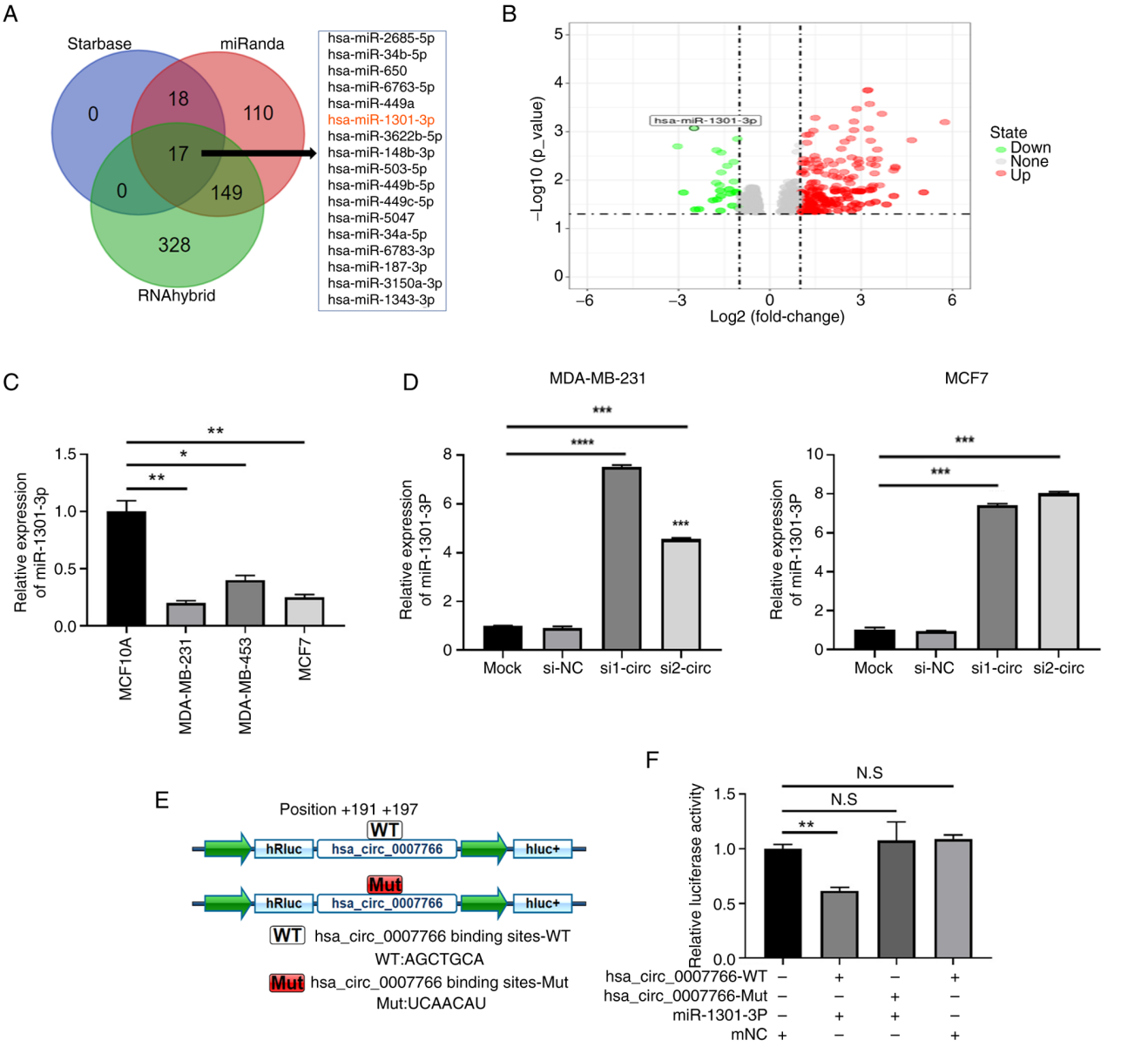


Figure 3. hsa_circ_0007766 acts as a miR-1301-3p sponge in BC cells. (A) A total of 11 potential target miRNAs of hsa-circ-0007766 were predicted by bioinformatic analysis. (B) The volcano plot depicts the expression of miR-1301-3p between BC tissues and tumor-adjacent normal tissues. The x-axis represents the log2 fold change, and the y-axis represents the-log10 P-value. (C) The expression levels of miR-1301-3p in BC cell lines were determined using RT-qPCR. (D) RT-qPCR was utilized to assess the expression of miR-1301-3p following the downregulation of hsa_circ_0007766. (E) A schematic illustration depicted the hsa_circ_0007766 Luciferase reporter vector, both wild-type and mutant type, at the binding site with miR-1301-3p. (F) A dual-luciferase reporter assay was conducted to verify the interaction between hsa_circ_0007766 and miR-1301-3p. *P<0.05, **P<0.01, ***P<0.001 and ****P<0.0001. miR or miRNA, microRNA; BC, breast cancer; RT-qPCR, reverse transcription-quantitative PCR; si-, small interfering; NC, negative control; N.S., no significance; WT, wild-type; Mut, mutant.

assays were conducted to further verify the binding between miR-1301-3p and DNMT3B mRNA [3'-untranslated region (UTR) of wild or mutant fragments]. The DNMT3B luciferase reporter vector (wild type and mutant type) for the binding site with miR-1301-3p was synthesized and constructed by Guangzhou RiboBio Co., Ltd. The results showed that miR-1301-3p could significantly decrease the relative luciferase activity of the wild-type luciferase reporter but not the mutant one (Fig. 5C and D).

Subsequently, miR-1301-3p mimics or inhibitors were transfected into MCF7 and MDA-MB-231 cells. Western blot analysis revealed that the expression of DNMT3B was significantly reduced upon transfection with miR-1301-3p mimics, whereas it was significantly increased following transfection with the miR-1301-3p inhibitor (Fig. 5E). Previous studies have demonstrated that miRNAs and DNA methyltransferases (DNMTs) are capable of forming a regulatory feedback loop (16,17). In line with this, shRNAs targeting DNMT3B were designed, which were synthesized by Guangzhou RiboBio Co., Ltd. To assess the efficacy of DNMT3B knockdown, RT-qPCR was employed to measure the relative expression levels of DNMT3B in BC cell lines after transfection with either a NC or the shRNA DNMT3B. The findings indicated a significant downregulation of DNMT3B expression in the shRNA-DNMT3B transfected cells compared with the NC group (Fig. S2). Furthermore, the

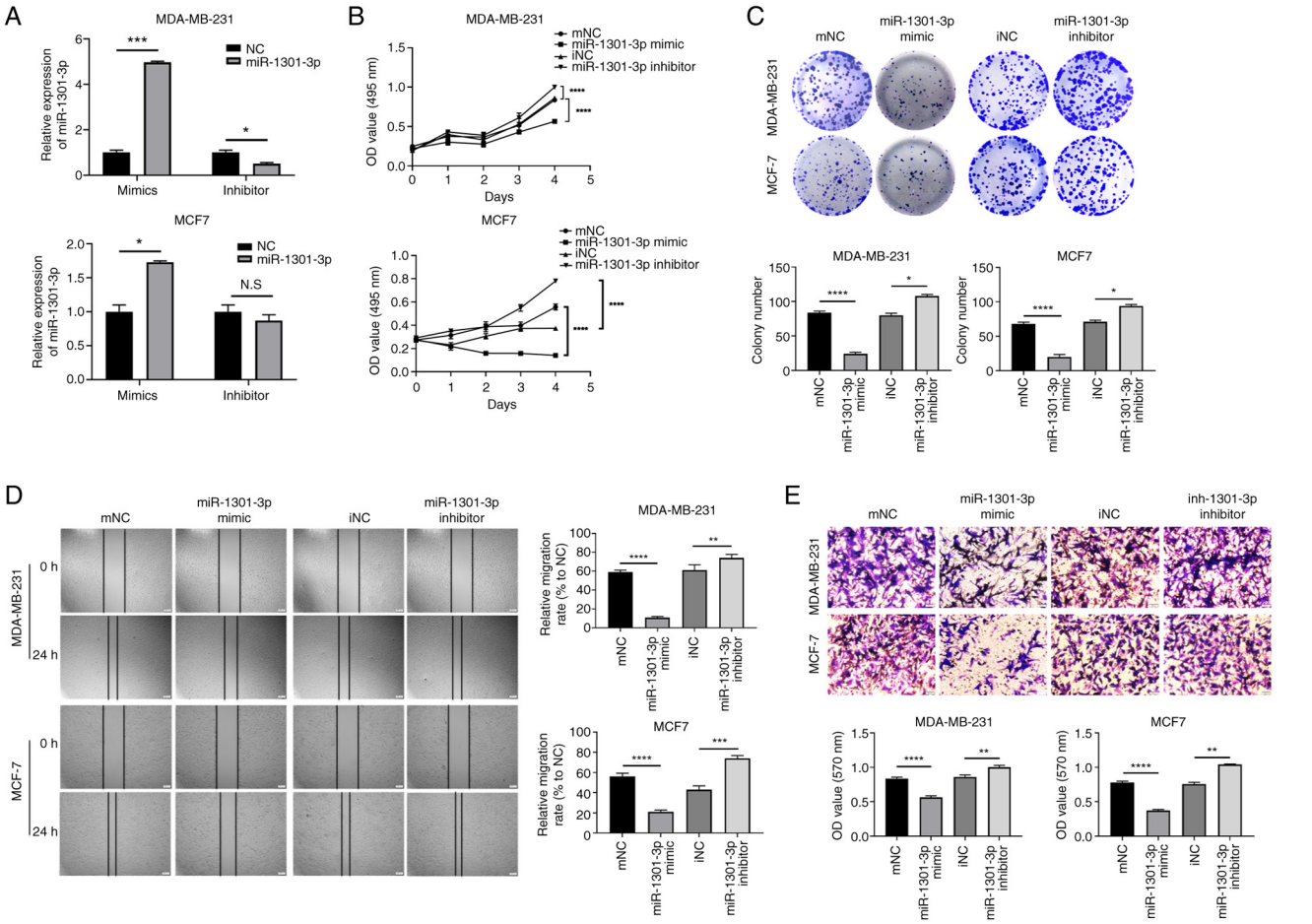


Figure 4. miR-1301-3p suppresses BC cells proliferation, migration and invasion *in vitro*. (A) The efficacy of miR-1301-3p was confirmed in BC cells following transfection with miR-1301-3p mimics or inhibitors, as determined by reverse transcription-quantitative PCR. (B and C) MTT assays and colony formation assays were employed to assess cell viability and colony-forming ability in BC cells transfected with NC and miRNA mimics or inhibitors. (D and E) Wound healing assays and Transwell Invasion assays were performed to evaluate cell migration and invasion of cells. *P<0.05, **P<0.01, ***P<0.001 and ****P<0.0001. Magnification, x100. Scale bar, 100 μm. miR or miRNA, microRNA; BC, breast cancer; NC, negative control; N.S., no significance.

expression levels of miR-1301-3p were examined by qPCR following DNMT3B silencing, and the results demonstrated that the knockdown of DNMT3B significantly upregulated miR-1301-3p expression in BC cells (Fig. 5F). In summary, these observations confirm the presence of a regulatory loop between miR-1301-3p and DNMT3B that plays a role in the development of BC.

Hsa-circ-0007766 modulates DNMT3B-mediated proliferation and metastasis through miR-1301-3p sponging in BC cells. To further elucidate the interplay among has_circ_0007766, miR-1301-3p and DNMT3B, a series of rescue experiments in MDA-MB-231 and MCF7 cell lines were conducted after co-transfecting si-hsa-circ-0007766 with the miR-1301-3p inhibitor. MTT assays, wound healing assays and Transwell invasion assays were employed to assess the regulatory effects between hsa_circ_0007766 and miR-1301-3p. The results indicated that the miR-1301-3p inhibitor significantly reversed the suppressive effects of si-hsa-circ-0007766 on cell proliferation, migration and invasion in BC cell lines (Fig. 6A-C).

To confirm the regulatory influence of hsa_circ_0007766 and miR-1301-3p on DNMT3B expression, MTT assays and wound healing assays were performed following co-transfection with sh-DNMT3B and either si-hsa_circ_0007766 or the miR-1301-3p inhibitor in BC cells. The results demonstrated that sh-DNMT3B significantly reduced the proliferation and migration capabilities in BC cells, with an enhanced effect observed when si-hsa_circ_0007766 and sh-DNMT3B were co-transfected (Fig. 6D and E). Additionally, the miR-1301-3p inhibitor significantly reversed the inhibitory effects of sh-DNMT3B on cell proliferation and migration in BC cell lines (Fig. 6D and E).

Collectively, the present findings suggest that hsa_circ_0007766 regulates the expression of DNMT3B by sponging miR-1301-3p, thereby playing a role in the proliferation, migration and invasion of BC cells. This regulatory mechanism provides insights into the complex interactions between circRNAs, miRNAs and DNMTs in the context of BC biology.

Discussion

A variety of circRNAs has been shown to regulate the onset and progression of cancer (18). An increasing body of research points to the dysregulated expression of circRNAs in BC, suggesting their involvement in tumorigenesis, development

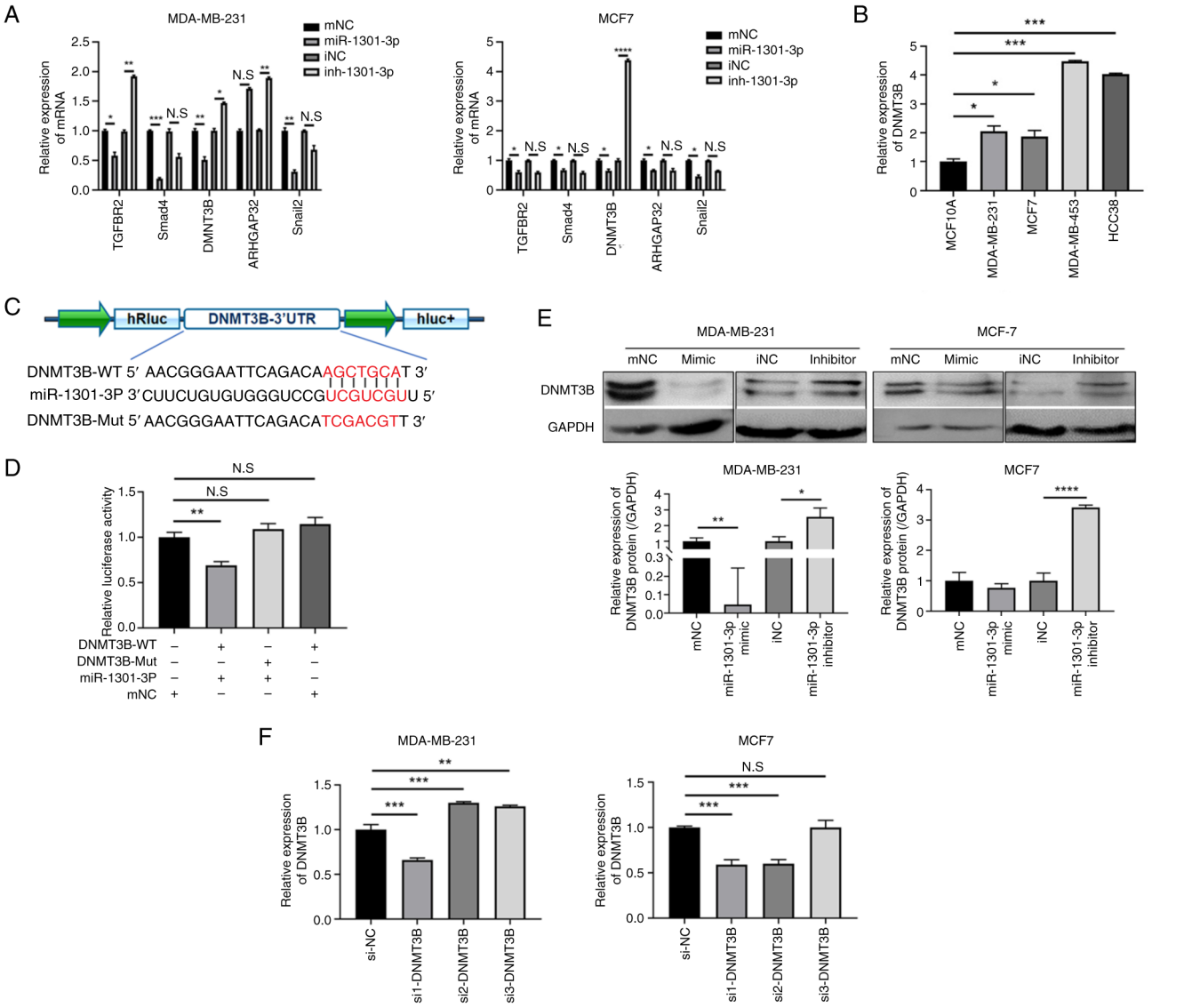


Figure 5. DNMT3B is a downstream target of miR-1301-3p and reciprocally regulates miR-1301-3p. (A) The target genes of miR-1301-3p were predicted. (B) The expression levels of DNMT3B were measured in normal breast cells and breast cancer cell lines using RT-qPCR. (C) A schematic illustration depicted the putative binding sites of the 3'UTR of DNMT3B (wild-type or mutant fragments) with miR-1301-3p. (D) A dual-luciferase reporter assay was conducted to confirm the interaction between DNMT3B and miR-1301-3p. (E) Western blot analysis demonstrated the effect of miR-1301-3p on DNMT3B expression. (F) The expression of miR-1301-3p was assessed by RT-qPCR following DNMT3B knockdown. *P<0.05, **P<0.01, ***P<0.001 and ****P<0.0001. DNMT3B, DNA methyltransferase 3B; miR, microRNA; NC, negative control; RT-qPCR, reverse transcription-quantitative PCR; UTR, untranslated region; sh-, short hairpin; NC, negative control; N.S., no significance.

and metastasis. The mechanistic roles of circRNAs in BC are primarily characterized by their function as ceRNAs or miRNA sponges (10,19). Moreover, circRNAs have been implicated in protein translation, regulation of protein binding, and modulation of gene transcription (20,21).

In the present study, a significant increase in the expression of hsa_circ_0007766 in BC tissues and cell lines was identified through bioinformatics software prediction and RT-qPCR detection. Silencing hsa_circ_0007766 in BC cells led to a notable inhibition of cell proliferation, invasion and migration, as well as a decrease in the protein expression of PCNA and Vimentin, and an increase in E-cadherin, aligning with previous findings (13), which suggests a potential role for hsa_circ_0007766 in BC tumorigenesis.

miRNAs that bind to hsa_circ_0007766 were screened and identified using bioinformatics tools and RT-qPCR. miR-1301-3p was found to be downregulated in BC cell lines, and its expression was significantly upregulated after silencing hsa_circ_0007766 with siRNA. Dual-luciferase reporter assays were employed to validate this interaction. miR-1301-3p has been reported to play promotional or inhibitory roles in tumor progression across different cancer types, including BC (22-24). Functional assessment of miR-1301-3p, through the transient transfection of miR-1301-3p mimic or inhibitor in BC cells, revealed that the mimic significantly suppressed cell proliferation, migration and invasion, while the inhibitor had opposite effects, indicating an antitumor role for miR-1301-3p in BC cells.

Studies have shown the existence of a regulatory loop between miRNA expression and epigenetic modifications (17,25,26). DNMTs can downregulate miRNA expression through methylation in the promoter region of miRNAs, and

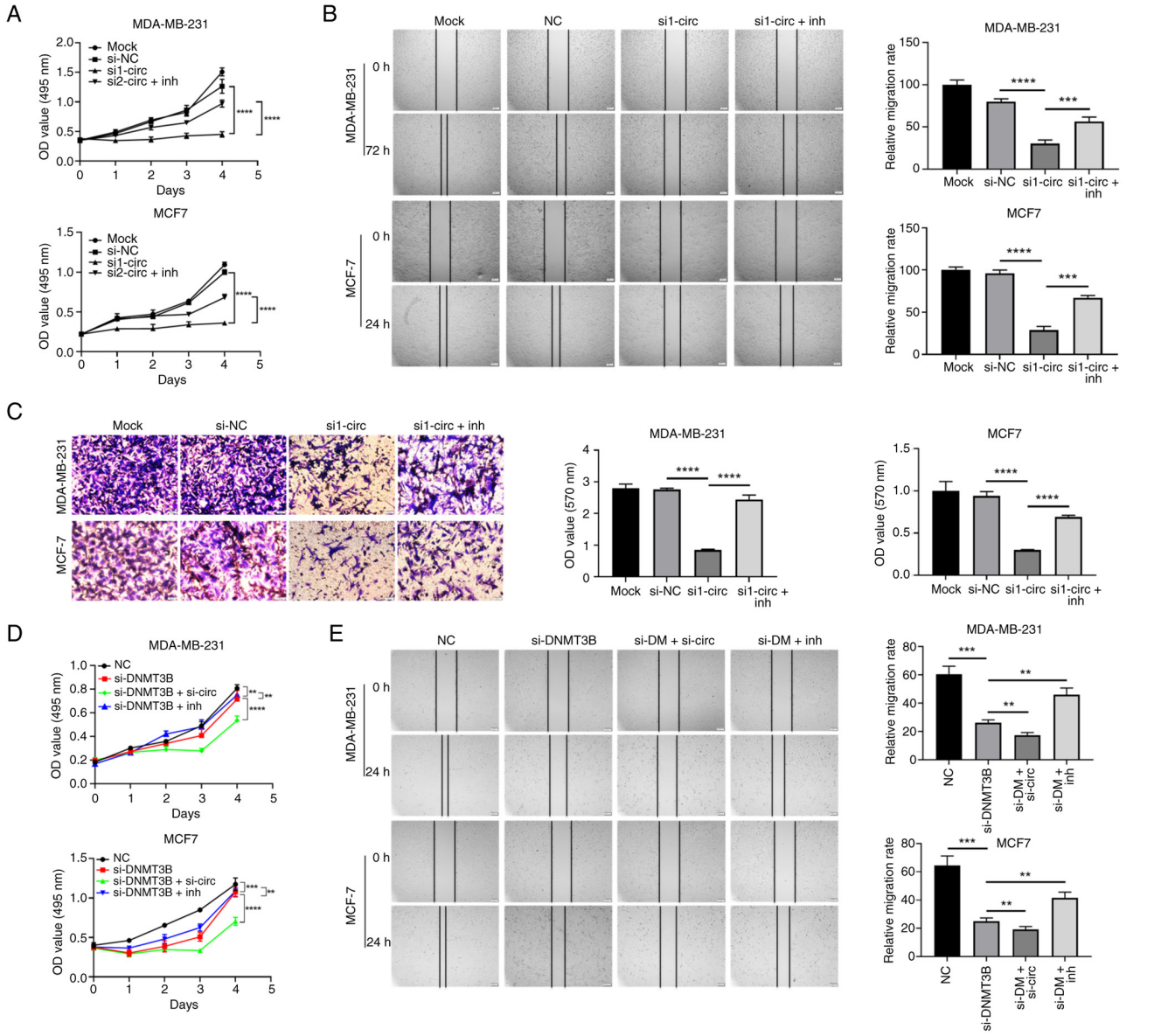


Figure 6. hsa_circ_0007766/miR-1301-3p/DNMT3B axis regulates proliferation, migration and invasion in BC cells. (A) Cell proliferation was detected by MTT assay following transfection or co-transfection with si-hsa_circ_0007766, miR-1301-3p inhibitor. (B and C) The migration and invasion capabilities of BC cells, transfection or co-transfection with si-hsa_circ_0007766 and miR-1301-3p inhibitor, were quantified using wound healing assays and Transwell invasion assays, respectively. (D and E) The proliferation and migration abilities of BC cells, transfection or co-transfection with sh-DNMT3B, si-hsa_circ_0007766, or miR-1301-3p inhibitor, were measured by MTT assays and wound healing assays, respectively. **P<0.01, ***P<0.001 and ****P<0.0001. Magnification, x100. Scale bar, 100 μm. DNMT3B, DNA methyltransferase 3B; BC, breast cancer; miR, microRNA; sh-, short hairpin; NC, negative control; N.S., no significance.

miRNAs can inhibit the expression of DNMTs by targeting the 3'-UTR region of DNMTs (17,27,28). A previous study by the authors found that the promoter region of miR-1301-3p was hypermethylated in BC cells, and the demethylation drug, decitabine significantly reduced the methylation level of the miR-1301-3p promoter and enhanced miR-1301-3p expression, suggesting that low miR-1301-3p expression in BC cells may be related to methylation regulation. Hypermethylation of CpG-rich promoter regions of tumor suppressor miRNAs typically leads to their silencing via DNMTs (29). Conversely, these miRNAs can also target DNMTs to inhibit their expression (15).

To elucidate the molecular mechanisms by which miR-1301-3p exerts a tumor suppressor role in BC, bioinformatics analysis was employed to identify mRNAs that bind to miR-1301-3p. Building on the authors' previous research, DNMT3B was identified as a potential downstream target gene of miR-1301-3p. DNMT3B, a key DNMT, is predominantly involved in the *de novo* methylation of CpG sites during DNA methylation processes (30). Evidence suggests that DNMT3B is often overexpressed in patients with BC and is inversely associated with patient survival rates (31,32). However, the inhibition of DNMT3B has been shown to suppress the metastasis of BC cells. Several miRNAs have been demonstrated to target DNMT3B, thereby influencing DNA methylation patterns (33). In the present study, it was observed that DNMT3B was highly expressed in BC cells, inversely correlating with miR-1301-3p levels. Dual-luciferase reporter assays were utilized to confirm the interaction between DNMT3B and miR-1301-3p. Additionally, western blot analysis was

conducted to validate that the overexpression of miR-1301-3p could downregulate the expression of DNMT3B protein. Notably, the inhibition of DNMT3B significantly upregulated the expression of miR-1301-3p. These findings demonstrate the presence of a regulatory feedback loop between miR-1301-3p and DNMT3B, which modulates the methylation level of the miR-1301-3p promoter region.

Subsequently, rescue experiments were conducted to verify the interplay and mutual regulatory relationship among hsa_circ_0007766, miR-1301-3p and DNMT3B. The findings demonstrated that the miR-1301-3p inhibitor could significantly counteract the suppressive effects of si-hsa_circ_0007766 on the proliferation, migration and invasion of BC cells. Notably, BC cells transfected solely with sh-DNMT3B showed a pronounced inhibition of cellular proliferation, migration and invasion. This inhibitory effect was further enhanced when co-transfected with si-hsa_circ_0007766. However, co-transfection with the miR-1301-3p inhibitor abrogated this enhancement. Moreover, the knockdown of hsa_circ_0007766 led to a decrease in DNMT3B expression, but this was reversed with a significant increase in DNMT3B expression upon co-transfection of si-hsa_circ_0007766 and the miR-1301-3p inhibitor. Collectively, these results suggest that hsa_circ_0007766 modulates DNMT3B expression by acting as a sponge for miR-1301-3p, thereby influencing the proliferation, migration and invasion of BC cells. It is important to acknowledge that the regulatory mechanism of the hsa_circ_0007766/miR-1301-3p/DNMT3B axis is primarily based on *in vitro* studies in BC cell lines, with a paucity of animal or clinical evidence to support these findings.

In conclusion, hsa_circ_0007766 exhibits significant upregulation in BC and plays a pivotal role in regulating the proliferative, migratory and invasive capabilities of BC cells. Furthermore, hsa_circ_0007766 modulates the expression levels of DNMT3B by sponging miR-1301-3p. Additionally, the expression of miR-1301-3p is subject to regulation by DNA methylation, uncovering a novel positive feedback loop involving miR-1301-3p and DNMT3B within BC cells. The findings of the present study not only delve into the functional roles and underlying mechanisms of hsa_circ_0007766 in BC but also highlight its potential as a diagnostic and therapeutic target for the disease.

Acknowledgements

Not applicable.

Funding

The present study was supported by the Fundamental Research Funds for the Central Universities, the North Minzu University (grant no. 2025QNPY54), the High-level Talent Project of North Minzu University (grant no. 2025BG326) and the Ningxia Natural Science Foundation (2026AAC030319).

Availability of data and materials

The data generated in the present study may be requested from the corresponding author.

Authors' contributions

HY and YC conceived and designed the experiments. YLi, YLu and TY performed the experiments. YLi and YLu prepared figures and tables. HY, YC and YLu analyzed and interpreted the data. HY and YLi wrote the manuscript. HY and YC supervised the project. HY and YC confirm the authenticity of all the raw data. All authors read and approved the final version of the manuscript.

Ethics approval and consent to participate

Not applicable.

Patient consent for publication

Not applicable.

Competing interests

The authors declare that they have no competing interests.

References

1. Gu H, Wang R, Beeraka NM, Lu P, Zhao X, Li L, Liu Y, Kandula DR, Fan R, Gayathri T, *et al*: Global burden and trends of breast cancer: GLOBOCAN 2022 estimates of incidence and mortality in 185 countries. Chin Med J (Engl) 139: 404-414, 2026.
2. Siegel RL, Giaquinto AN and Jemal A: Cancer statistics, 2024. CA Cancer J Clin 74: 12-49, 2024.
3. Yang J, Li Y, Wang Z, Sun Y, He Y, Niu T, Liang Y, Chen X, Chen T, Han D, *et al*: CircKIAA1617 promotes stemness via USP14/PGRMC1-mediated autophagy and lipid metabolism reprogramming in ER-positive breast cancer. Mol Cancer 25: 55, 2026.
4. Palcau AC, Pulito C, De Pascale V, Casadei L, Valerio M, Sacconi A, Canu V, Rutigliano D, Donzelli S, Sardo FL, *et al*: CircPVT1 weakens miR-33a-5p unleashing the c-MYC/GLS1 metabolic axis in breast cancer. J Exp Clin Cancer Res 44: 100, 2025.
5. Tan Z, Boyapati K, Tressler CM, Jenkinson NM and Glunde K: Glutamine transporter SLC38A3 promotes breast cancer metastasis via Gsk3β/β-catenin/EMT pathway. Cancer Lett 586: 216653, 2024.
6. Goodall GJ and Wickramasinghe VO: RNA in cancer. Nat Rev Cancer 21: 22-36, 2021.
7. Hansen TB, Jensen TI, Clausen BH, Bramsen JB, Finsen B, Damgaard CK and Kjems J: Natural RNA circles function as efficient microRNA sponges. Nature 495: 384-388, 2013.
8. Meng S, Zhou H, Feng Z, Xu Z, Tang Y, Li P and Wu M: CircRNA: Functions and properties of a novel potential biomarker for cancer. Mol Cancer 16: 94, 2017.
9. Wang X, Yang X, Xing L, Chen H, Xie F, Wang B, Shi B, Yang Y and Chen J: CircLRBA promotes epithelial-mesenchymal transition, immune evasion, chemoimmunotherapy resistance and metastasis through stabilizing Twist1. Adv Sci (Weinh) 12: e08918, 2025.
10. Ren J, Chen W, Zhou Y, Sun J and Jiang G: The novel circRNA circ_0045881 inhibits cell proliferation and invasion by targeting mir-214-3p in triple-negative breast cancer. BMC Cancer 24: 278, 2024.
11. Zhang S, Xia W, Dong G, Xu W, Li M and Xu L: Cyclic RNA molecule circ_0007766 promotes the proliferation of lung adenocarcinoma cells by up-regulating the expression of Cyclin D1/CyclinE1/CDK4. Zhongguo Fei Ai Za Zhi 22: 271-279, 2019 (In Chinese).
12. Xu W, Zhou B, Wu J, Jiang P, Chen H and Yan F: Circular RNA hsa-circ-0007766 modulates the progression of Gastric Carcinoma via miR-1233-3p/GDF15 axis. Int J Med Sci 17: 1569-1583, 2020.

13. Li J, Ma M, Yang X, Zhang M, Luo J, Zhou H, Huang N, Xiao F, Lai B, Lv W and Zhang N: Circular HER2 RNA positive triple negative breast cancer is sensitive to Pertuzumab. Mol Cancer 19: 142, 2020.
14. Zhang M, Bai X, Zeng X, Liu J, Liu F and Zhang Z: circRNA-miRNA-mRNA in breast cancer. Clin Chim Acta 523: 120-130, 2021.
15. Livak KJ and Schmittgen TD: Analysis of relative gene expression data using real-time quantitative PCR and the 2(-Delta Delta C(T)) method. Methods 25: 402-408, 2001.
16. Pang Y, Liu J, Li X, Xiao G, Wang H, Yang G, Li Y, Tang SC, Qin S, Du N, *et al*: MYC and DNMT3A-mediated DNA methylation represses microRNA-200b in triple negative breast cancer. J Cell Mol Med 22: 6262-6274, 2018.
17. Ma L, Li C, Yin H, Huang J, Yu S, Zhao J, Tang Y, Yu M, Lin J, Ding L and Cui Q: The mechanism of DNA methylation and miRNA in breast cancer. Int J Mol Sci 24: 9360, 2023.
18. Conn VM, Chinnaiyan AM and Conn SJ: Circular RNA in cancer. Nat Rev Cancer 24: 597-613, 2024.
19. Zhang C, Yu Z, Yang S, Liu Y, Song J, Mao J, Li M and Zhao Y: ZNF460-mediated circRPPH1 promotes TNBC progression through ITGA5-induced FAK/PI3K/AKT activation in a ceRNA manner. Mol Cancer 23: 33, 2024.
20. Huang D, Zhu X, Ye S, Zhang J, Liao J, Zhang N, Zeng X, Wang J, Yang B, Zhang Y, *et al*: Tumour circular RNAs elicit anti-tumour immunity by encoding cryptic peptides. Nature 625: 593-602, 2024.
21. Yang B, Wang YW and Zhang K: Interactions between circRNA and protein in breast cancer. Gene 895: 148019, 2024.
22. Qiao DH, He XM, Yang H, Zhou Y, Deng X, Cheng L and Zhou XY: miR-1301-3p suppresses tumor growth by downregulating PCNA in thyroid papillary cancer. Am J Otolaryngol 42: 102920, 2021.
23. Peng X, Yan B and Shen Y: MiR-1301-3p inhibits human breast cancer cell proliferation by regulating cell cycle progression and apoptosis through directly targeting ICT1. Breast Cancer 25: 742-752, 2018.
24. Song XL, Huang B, Zhou BW, Wang C, Liao ZW, Yu Y and Zhao SC: miR-1301-3p promotes prostate cancer stem cell expansion by targeting SFRP1 and GSK3β. Biomed Pharmacother 99: 369-374, 2018.
25. Pronina IV, Loginov VI, Burdennyy AM, Fridman MV, Senchenko VN, Kazubskaya TP, Kushlinskii NE, Dmitriev AA and Braga EA: DNA methylation contributes to deregulation of 12 cancer-associated microRNAs and breast cancer progression. Gene 604: 1-8, 2017.
26. Chen ZH, Chen YB, Yue HR, Zhou XJ, Ma HY, Wang X, Cao XC and Yu Y: PAX5-miR-142 feedback loop promotes breast cancer proliferation by regulating DNMT1 and ZEB1. Mol Med 29: 89, 2023.
27. Tao S, Li H, Ma X, Lian B, He J, Gao Y and Li J: Methylation-mediated silencing of MicroRNA-497 promotes breast cancer progression through up-regulation of Mucin1. Front Oncol 10: 552099, 2020.
28. Shi W, Tang T, Li X, Deng S, Li R, Wang Y, Wang Y, Xia T, Zhang Y, Zen K, *et al*: Methylation-mediated silencing of miR-133a-3p promotes breast cancer cell migration and stemness via miR-133a-3p/MAML1/DNMT3A positive feedback loop. J Exp Clin Cancer Res 38: 429, 2019.
29. Chatterjee B, Ghosh K, Swain A, Nalla KK, Ravula H, Pan A and Kanade SR: The phytochemical brazilin suppress DNMT1 expression by recruiting p53 to its promoter resulting in the epigenetic restoration of p21 in MCF7cells. Phytomedicine 95: 153885, 2022.
30. Jurkowska RZ, Jurkowski TP and Jeltsch A: Structure and function of mammalian DNA methyltransferases. Chembiochem 12: 206-222, 2011.
31. So JY, Yang HH, Park WY, Skrypek N, Ishii H, Chen JM, Lee MP and Yang L: DNA Methyltransferase 3B-mediated intratumoral heterogeneity and therapeutic targeting in breast cancer recurrence and metastasis. Mol Cancer Res 20: 1674-1685, 2022.
32. Vitte AL, Chuffart F, Jacquet E, Nika E, Mousseau M, Jung I, Tabone-Eglinger S, Bachelot T, Rousseaux S, Khochbin S and Bourova-Flin E: Discovery of epigenetically silenced tumour suppressor genes in aggressive breast cancer through a computational approach. NAR Cancer 7: zcaf020, 2025.
33. TangX,TuG,YangG,WangX,KangL,YangL,ZengH,WanX,QiaoY, Cui X, *et al*: Autocrine TGF-β1/miR-200s/miR-221/DNMT3B regulatory loop maintains CAF status to fuel breast cancer cell proliferation. Cancer Lett 452: 79-89, 2019.

Copyright © 2026 Yang et al. This work is licensed under a Creative Commons Attribution-NonCommercial-NoDerivatives 4.0 International (CC BY-NC-ND 4.0) License.